PHYSICAL REVIEW B VOLUME 18, NUMBER 8 15 OCTOBER 1978

Mott distortion of the electron-hole fluid phase diagram

G. A. Thomas, J. B. Mock, and M. Capizzi *
Bell Laboratories, Murray Hill, New Jersey 07974
(Received 23 May 1978)

Spectroscopic measurements of the electron-hole fluid in Ge indicate that the liquid-gas phase diagram is distorted from that of simple fluids. This Mott distortion appears as a broadening of the top of the phase diagram with gas densities at least a factor of 3 lower than expected in the region near the Mott density. The precise shape of the phase boundary in the high-density gas remains uncertain because of inadequacies in our theoretical and experimental understanding of screening effects at finite temperatures. However, no first-order Mott transition separate from the liquid-gas transition is found to occur.

I. INTRODUCTION

Two phase transitions occur at once in photoexcited semiconductors at low temperatures when the metallic electron-hole liquid condenses from the insulating exciton gas.[1] One of these transitions is the liquid-gas and the other is the metal-insulator. In 1943, Landau and Zeldovich[2] discussed the possibility, in principle, of these two phase transitions occurring separately in the case of liquid mercury. However, both transitions have never been observed separately in the same system.[3]

The electron-hole fluid is an unusually good candidate[4] for a system in which such a separation might occur. On the one hand, based on the arguments of Mott,[3] one would expect the characteristic density for the metal-insulator transition to be that for which the screening length is of the order of the excition Bohr radius. On the other hand, the critical density for the liquid-gas phase transition occurs[5] where the interparticle spacing is of the order of the exciton Bohr radius. Because of the light mass of the electrons and holes and because both can participate in the screening, the Mott density, using either the Debye-Hückel or Fermi-Thomas screening lengths, occurs over an order of magnitude below[6] the e-h liquid critical density. In contrast, these densities are comparable in mercury and other liquid metals.[3]

Although the possibility of two separate critical points was not considered in the first measurements of the e-h liquid critical point,[5] a number of theoretical discussions have been presented including the extensive work by Ebeling, Kraeft, and Kremp,[7] and papers by Rice,[4] by Insepov, Norman, and Shurova,[8] and by Sander and Fairobent.[9] Later experimental studies[6,10] suggested that the metal-insulator transition might play a role in determining the shape of the liquid-gas phase diagram but were unable to complete the picture. The possible presence of e-h plasma in the gas phase was also noted by Timusk,[11] Shah, Dayem, and Worlock,[12] and Miniscalco, Huang, and Salamon.[13]

It now appears that the luminescence from the gas phase, which has been the source of all of the experimental studies cited above, can be described by a combination of trions, excitonic molecules, and excitons at densities above the Mott criterion in germanium.[14] This model is based upon the uncertain approximations of considering the strongly interacting gas in terms of bound states and bands in the continuum which are rigidly shifted by screening effects. However, this model provides the first quantitative description of the luminescence spectrum and the gas densitites in the region of the phase diagram near the Mott transition. Based on these surprising results we have been able to extend the spectroscopically determined gas phase boundary by about an order of magnitude in density. The nearly complete phase boundary then suggests that, although a separate Mott transition does not not occur, there is a substantial distortion of the phase diagram from that of simple fluids, an effect which we refer to as a Mott distortion.

In Sec. II, we present a description of the experimental apparatus. In Sec. III, we proceed through the construction of the phase diagram and present the evidence for a Mott distortion, with conclusions presented in Sec. IV.

II. EXPERIMENTAL APPARATUS AND PROCEDURES

The most important aspects of the experimental effort to delineate the phase diagram of the e-h fluid are the spatial distribution of the e-h pair density and temperature within the sample. In earlier studies,[5,6] the surface of a large sample has usually been excited to obtain densities near the liquid critical density. However, slightly lower densities in the gas can be attained with the temperature under control using a nearly uniform carrier density distribution in a surface-excited

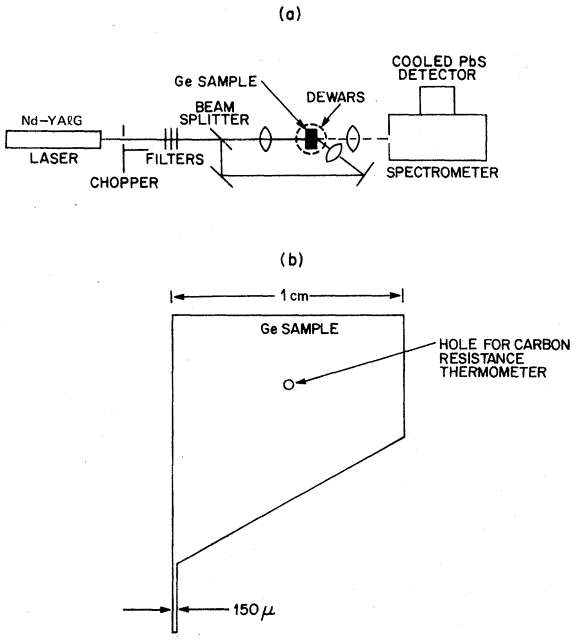

FIG. 1. Experimental apparatus. (a) Schematic diagram indicating the conventional luminescence setup, but with excitation of the sample on both sides using a split, 1.06-μm Nd-YAlG laser beam. (b) Cross-sectional view of one of the samples used to obtain a nearly homogeneous spatial distribution of photoexcited electrons and holes.

thin sample.[10,14] We discuss here our general apparatus and the thin samples used for the latter case.

Figure 1(a) shows a schematic sketch of the equipment indicating first, the Nd-YAlG laser, operated cw at a wavelength of 1.06 μm and a power of 5 W, used to photoexcite the e-h pairs. Before hitting the sample the beam was chopped at 13 Hz, filtered to remove the quartz-iodide excitation light and to reduce the intensity, split into two beams of equal intensity, and finally focussed onto opposite sides of the sample. The sample was cooled in a glass chamber of He exchange gas, surrounded by superfluid ^{4}He, vacuum chambers, and liquid nitrogen. The luminescence was collected from the sample with a lens and focused into a Bausch and Lomb 50-cm grating monochromator with $f/4.4$ optics and with a grating blazed at a wavelength of 1.8 μm. The output of the spectrometer was detected with a selected PbS detector, with cold cap and filters, cooled to 172 K with liquid Freon 13. The detector output was preamplified and fed into a PAR 124 lock-in amplifier and then to a chart recorder. The spectrometer wavelength was monitored electronically and also put into the chart recorder with a signal accurately linear in wavelength.

For bulk sample pumping, near-hemisphere samples were used as described previously.[6] However, in an attempt to obtain nearly uniform carrier distributions, a bulk sample of purity $n_D - n_A \sim 10^{10}$ cm^{-3}, dislocation free, with a thin tail was used as illustrated in Fig. 1(b). The flat tail in several samples was approximately of dimensions $10 \times 2 \times 0.15$ mm^3, with both sides ground flat, polished heavily with Syton and then etched[6] with CP-4A (5 parts HNO_3, 3 parts HF, and 3 parts glacial acetic acid). A hole was ground in the bulk part of the sample away from the tail, as shown in Fig. 1(b), to allow a carbon thermometer to be glued inside with GE7031 varnish. The ends of the hole were covered with small Ge crystals sealed in place with the same adhesive. In this way the outer surface of the sample was cooled by convection of the He gas, while the thermometer maintained its primary thermal contact to the sample by conduction.

In the measurements discussed below which were performed on bulk samples, we were able to detect no temperature difference between the thermometer and the excitation region within our measurement accuracy ($\lesssim 0.02$ K, lowest accuracy for $T \gtrsim 15$ K). Checks were performed using the e-h liquid luminescence lineshape as a thermometer at powers up to 50 mW. A worst-case model[15] can be constructed to understand this accurate temperature sensing with a calculation of the spatial temperature distribution. A sphere of Ge with thermal conductivity $K_T = 10$ W/cm K and an outer surface (radius $b = 0.5$ cm) at 7 K will have a temperature rise ΔT on an inner sphere (of radius a) that is a source of heat of magnitude Q: $\Delta T = Q(b-a)/4\pi K_T ab$. This result indicates that a temperature rise, which would fall off as $1/r$, would be discernible if a small enough excitation spot was used. For our smallest spots ($a = 0.2$ mm), we would expect $\Delta T \lesssim 0.02$ K at input powers of 50 mW. Furthermore, we expect the real ΔT to be less than the model because of cooling along the flat, photoexcited sample face.

For the samples with thin tails (thickness ~ 150 μm) we observed measurable heating for the laser spot far enough on the tail from the bulk part of the sample. We tested temperature differences in this case using the e-h liquid onset as well as the lineshape, while moving the excitation spot from the bulk along the tail. We were able to position the beam, in all cases for the data presented below, so that the bulk-tail temperature difference was $\lesssim 0.1$ K, provided that the laser power was restricted. Because of this constraint on the laser power (related partly to surface recombination) we were only able to attain densities $n \sim 10^{16}$ cm^{-3} in the thin tails, whereas in the case of surface

pumping of bulk samples we were able to maintain peak densities $n \sim 10^{17}$ cm^{-3}.

The spatial distribution of carrier density was our second major source of concern. In the bulk samples the nonuniformity was substantial and complicated any analysis of the phase diagram. Studies of the spatial distribution in this case have been carried out by a number of authors[16] and are reviewed in Ref. 1. Within the thin tail the approach to homogeneity is substantially better.[10,14] Routinely, we have used spot sizes several times bigger than the bulk exciton diffusion length,[1,16] $L_D = 0.5$ mm. Here, we assume that the density will have an essentially one-dimensional variation near the spot center and will vary as $n = n_0 e^{-x/L_D}$, decreasing from both equally excited surfaces along the direction x perpendicular to the surface. A small, square entrance slit was used at the spectrometer, with an image size of the slit on the sample of 0.11×0.11 mm^2. As a result, luminescence from the excited region away from the spot center was excluded from the observed spectra. The density in the region observed will then vary as $n = n_0(e^{-x/L_D} + e^{-(W-x)/L_D})\big|_{x \le W}$, as illustrated in Fig. 2. This variation could in principle be used to refine the data analysis, assuming, of course, that this simple form is not modified substantially by surface recombination. However for a thickness $W = 150$ μm and $L_D = 0.5$ mm, the drop in density between the surface and the sample center will be 1.1% in the ideal case so that we can neglect it with better justification than that with which it is usually neglected.

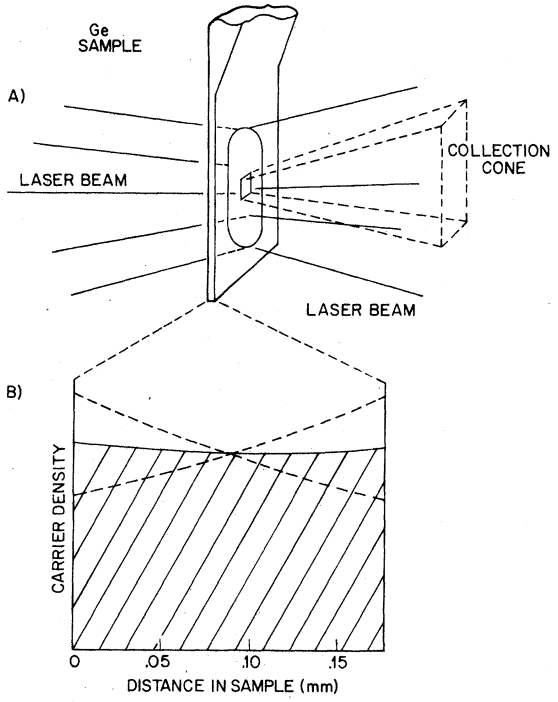

FIG. 2. Detail of sample excitation scheme. (a) Thin sample tail with large, uniform excitation spots on both sides and a small collection cone. The square is an image of the restricted spectrometer entrance slit. (b) Idealized plot of the carrier density as a function of position within the thin tail as discussed in the text. It is expected that surface recombination will reduce the surface density from that shown but that the characteristic length for density variations will be the exciton-diffusion length. Dashed lines are contributions from each surface; solid line enclosing shaded area is renormalized total density distribution.

III. CONSTRUCTION OF THE EXPERIMENTAL PHASE DIAGRAM

We now discuss experimental measurements of the phase boundaries of the e-h fluid in Ge. The results of our determinations are summarized in Fig. 3 along with measurements from other sources. We shall review first the liquid densities for $T < 6.4$ K and then the gas densities along the phase boundary. We reiterate two major points regarding this analysis. First, both liquid and gas boundaries (below $T \approx 5.5$ K) are calculated on an equal footing from results of spectroscopic measurements. Second, there is considerable uncertainity in the density regions near T_c where the liquid and gas luminescence lines overlap.

We shall also present measurements of the gas density for temperatures in the range $5\text{ K} < T < T_c$ based on two methods of interpreting the luminescence spectra. The first of these is the somewhat uncertain use of onsets of luminescence signals from the e-h liquid as temperature is lowered at a set of constant excitation intensities in inhomogeneously pumped samples. The second is a calculation of the gas density equivalent to that for the excitons at $T < 5$ K, but including, in addition, the significant density of correlated electrons and holes, trions, and excitonic molecules. This calculation, given our analysis of the spectra in this regime, extends the phase boundary by nearly an order of magnitude, but not to densities above 10^{16} cm^{-3}.

The solid line in Fig. 3 which indicates the e-h liquid phase boundary is a least-squares fit to a series of points measured from the luminescence spectrum by Thomas, Rice, and Hensel[5] and by Thomas, Phillips, Rice, and Hensel.[17] This procedure follows the analysis initially used by Pokrovskii and Svistunova[18] and since used by a number of others for similar studies or refinements of measurements in Ge (Benoit à la Guillaume and Voos,[19] Lo,[20] Martin and co-workers,[21-23] and Thomas and Capizzi[24]; see also Ref. 1). The e-h liquid luminescence line is fit as described by

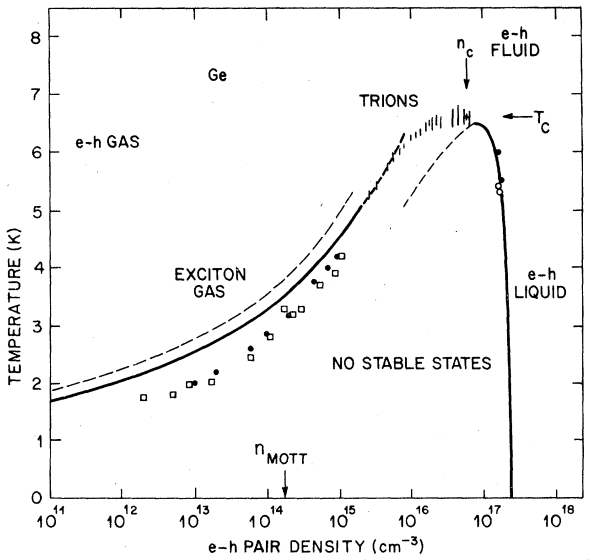

FIG. 3. Phase diagram of the electron-hole fluid showing equilibrium phase boundaries (solid lines) calculated from the spectroscopic measurements and the new portion of the phase boundary obtained by the same method including trions and excitonic molecules (heavy dashed line). Also shown are an alternative, equilibrium gas boundary for $\phi = 2.0$ meV (light dashed line at low n), and the gas-phase diagram for simple fluids (light dashed line near T_c). Measurements of onsets at high density (vertical bars, this work) are expected to closely approximate the equilibrium phase boundary, while those at lower density [open squares from Timusk (Ref. 11) and closed circles from Lo, Feldman, and Jeffries (Ref. 38)] differ from equilibrium as a result of hysteresis effects. The normalization of the high-temperature onsets in the density region of substantial trion contributions yields a revised estimate of the critical point at $T_c = 6.7 \pm 0.2$ K and $n_c = (6 \pm 1) \times 10^{16}$ cm^{-3}, as shown. Below $T \sim 3$ K the e-h fluid system does not approach equilibrium as closely as above because of lifetime effects. As a result the gas densities outside the e-h liquid under most experimental conditions will be closer to data points shown than to the thermodynamic phase diagram.

these authors and, from the fit, combined with the condition that the densities of electrons and holes be equal, the electron Fermi energy E_{Fe} is determined (as well as the value for holes E_{Fh}). With this result, and the fact that the fit is reasonably successful with a square-root density of states, we can calculate the electron density (equal to the e-h pair density).

A general formula for the particle density, which can be used for the liquid case here as well as for the gas constituents that we shall consider below, can be written

$$n = \sum_{i=1}^{m} \int_0^\infty d\epsilon \mathfrak{D}_i(\epsilon) f_i(\epsilon - \mu + \epsilon_i^0), \tag{1}$$

where the index i represents different types of particles, the energy ϵ is measured relative to the bottom of the band ϵ_i^0 for the particle considered, $\mathfrak{D}_i(\epsilon)$ is the density of states, f_i is the distribution function, and μ is the chemical potential for the entire system. This equation is the source of the estimates that we believe to provide the best current values of density along the e-h fluid phase boundary as shown by the solid lines in Fig. 3.

For the e-h liquid we need consider only one term in Eq. (1), that due to the electrons (or equivalently the holes). For this case the density of states is given by

$$\mathfrak{D}_1(\epsilon) = (g_1/2\pi^2)(2m_{de}/\hbar^2)^{3/2} \epsilon^{1/2}, \tag{2}$$

where the degeneracy $g_1 = 4$, the density of states mass $m_{de} = 0.22 m_0$, and m_0 is the free-electron mass. The distribution function is the Fermi function with the characteristic energy (determined from the luminescence line shape fitting as noted above)

$$\mu - \epsilon_e^0 = E_{Fe}. \tag{3}$$

With these formulae we can evaluate Eq. (1) to obtain the liquid density, but let us first consider briefly the values of m_{de} and E_{Fe} to be used. Thomas and Capizzi[24] have pointed out that the LO, as well as the LA, phonon replica contributes to the principal e-h liquid luminescence line in Ge and that, including both, the best values of E_{Fe} and E_{Fh} are reduced from those of Thomas, Rice and Hensel[5] by 3%. Previously Martin[22,23] obtained a good fit to the TA replica (which is completely resolved) and suggested that E_{Fe} was smaller than the value above by 4%. Similar analysis of the TA replica by Thomas and Capizzi yielded a reduction of 3%. Rice[25] has found that the density calculated from E_{Fe} will be modified by an enhancement in m_{de} due to many-body renormalization effects in the e-h liquid. Martin *et al.*[22] and Störmer[26] have found that such an enhancement is required to fit the dependence of the luminescence spectrum on magnetic field. Not including the LO replica, their analysis suggests a 10% larger m_{de}. The inclusion of the LO replica in this analysis will not appreciably modify the fitting since relatively sharp features in the LA replica were considered. Combining this increase in n at $T = 0$ with the above decreases in n from E_{Fe}, we estimate a net increase of ≈12% over the results of Ref. 5 so that

$$n_L(T = 0) = (2.6 \pm 0.1) \times 10^{17}\ cm^{-3}, \tag{4}$$

where we have estimated the uncertainty to try to include the systematic variations discussed above. The data of Ref. 5 has been shifted by a constant factor in Fig. 3 to coincide with this value of $n_L(T = 0)$.

Also shown in Fig. 3 along the liquid phase boundary are some density measurements above $T = 4.2$ K obtained from the luminescence spectrum by Martin,[27] solid circles. Up to a temperature of 6 K, both Thomas *et al.*[5] and Martin[27] observe a large thermal expansion as expected from theory. Miniscalco *et al.*[28,29] do not observe such a density reduction so we have only plotted their results at low-pumping levels (open circles). Martin has also extrapolated his measurements of E_{Fe} and E_{Fh} into the temperature region near the critical point and this estimate gives a value of $n = 1.1 \times 10^{17}$ cm^{-3} at $T = 6.5$—close to the solid line in Fig. 3. He estimated that T_c is between 6.7 and 7.7 K, and we would suggest that T_c is near the lower edge of this range because of the problem presented by density gradients within the sample. Another argument, presented by Martin[27] for a lower T_c is that he used the exciton line shape with an approximate density of states as a measure of the temperature and found that the resulting T values were systematically too high.

Severe density gradients are present in samples in which the carriers are created by surface photoexcitation, and these gradients introduce a serious complication into the analysis of the phase diagram near the critical point. In the experiments cited above,[5,28,29] the excitation source was a Nd-YAlG laser at $\lambda = 1.06$ μm, which is absorbed within about 1 μ of the surface, or a shorter-wavelength source.[27] On theoretical grounds we would expect that the compressibility of the e-h fluid would tend to diverge near T_c. Consequently, in this region it might be possible to create a high density e-h plasma gas that would resemble the e-h liquid in terms of its luminescence. Less of an effect would occur at higher or lower temperatures. The intensity of luminescence from a high-density plasma is amplified in the TA luminescence replica because the energy dependence of the forbidden matrix elements enhances recombination at large k values.[19,31]

Some luminescence spectra from the LA replicas which serve as examples of the density gradient problems are shown in Fig. 4. The laser pumping power is $P = P_0$, where P_0 is of the order of 50 mW. As can be seen from the data at $T = 6.56$ K and $T = 6.72$ K, it is tempting to analyze the spectra in terms of the presence of some liquid. However, we note that the most rapid change in the spectrum occurs when the sample is cooled to $T = 6.42$ K. Thomas *et al.*[5] have associated this rapid change with the liquid onset based on the expectation that some changes will occur above T_c due to the varying compressibility of the fluid and to fluctuations. Furthermore, we expect that the phase diagram will be flat near T_c, qualitatively similar to that

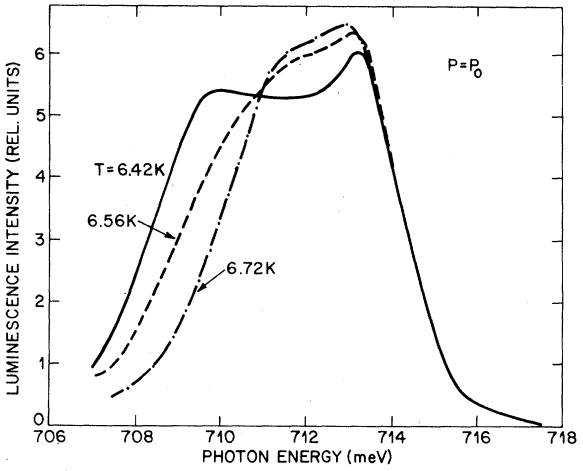

FIG. 4. Illustration of luminescence onset ambiguity present in defining the onset temperature. In this set of data the phase boundary is assumed to occur between $T = 6.72$ and 6.42 K, where the rapid variation in the line shape is occurring as shown. Luminescence from a region of high-density plasma is observed above T_c in this experiment because surface pumping of a large sample is used. These spectra define an onset data point as shown by a vertical bar in Fig. 3.

for simple fluids, so that a rapid change in the liquid density will occur as the temperature is lowered through T_c at constant P even with a substantial density gradient present. A second consequence of the relatively flat top of the phase diagram is that in this regime the onset temperatures should vary only slowly with pumping power. An observation of such nearly temperature-independent onsets is shown in the comparison of Figs. 4 and 5. In Fig. 5, a rapid change in the spectrum is observed between $T = 6.56$ and 6.42 K, as in Fig. 4, although the excitation intensity is lowered by about $\frac{1}{3}$.

Figures 4 and 5 also serve as examples of the onset measurements made along the gas phase boundary between 5 K and the critical region. The data shown, near T_c, are by far the most ambiguous from the point of view of determining the onset temperatures. At lower T, the difference between the liquid and gas densities rapidly becomes more clearly discernible as the two luminescence lines become increasingly separated. These onset measurements are shown as vertical bars in Fig. 3, with the bar length serving to represent an estimate of the uncertainty. As noted by Thomas *et al.*,[5] the densities of these onsets can only be estimated crudely in absolute terms, but the relative values are determined directly, provided that the density scales linearly with the pumping power. While such linearity is not present in thin samples,[30] due partly to strong surface recombination,

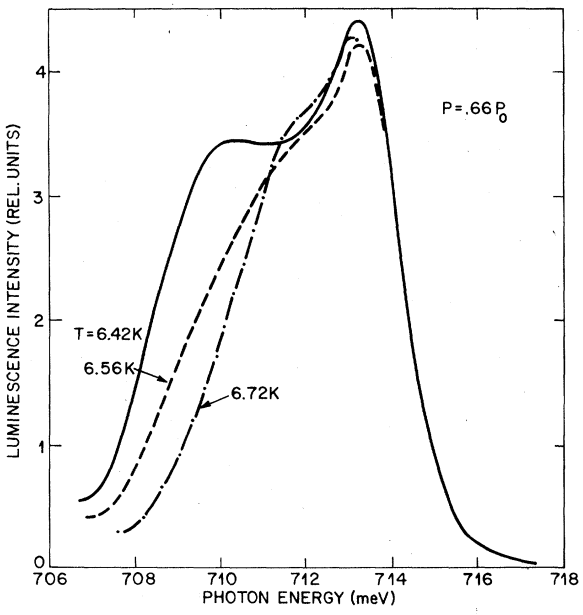

FIG. 5. Illustration of luminescence onset measurement as in Fig. 4, but at $\frac{1}{3}$ lower power. These two onsets are seen to occur at essentially the same temperature as is expected near the critical density. The onset temperature becomes increasingly better defined as density is lowered.

we find deviations to be small in the gas, away from T_c, in the large samples studied here. However, if such linearity held strictly it would be surprising because the lifetime of the correlated e-h fluid should vary with density.[1]

In the original measurements[5] of the phase diagram near T_c these high-temperature onsets were located in absolute density using the phase diagram for simple fluids. We can now relax that assumption using the model of the high-density gas proposed by Thomas and Rice[14] in terms of the absence of a Mott transition and the presence of trions and excitonic molecules. Based on that work we can calculate the gas densities for temperatures well above 4.2 K based on the spectroscopic measurements. Then we can use these spectroscopic densities to normalize the onset measurements at a temperature near $T = 5.5$ K as has been done in Fig. 3. We turn next to the method by which the spectroscopic gas densities are obtained and then shall return to a summary of the results and discuss the observation of a substantial deviation from the phase diagram for simple fluids in Sec. IV.

The solid line in Fig. 3 which indicates the exciton saturated vapor pressure in thermal equilibrium is constructed from the luninescence spectrum as discussed by Thomas, Frova, Hensel, Miller, and Lee,[6] i.e., it is calculated from the measured condensation energy of excitons and the density of states for free excitons, assuming thermal equilibrium. The line-shape analysis involved has been used in approximate form by a number of workers to analyze the exciton luminescence in Ge (Benoit à la Guillaume and Voos,[19] Lo,[20] and Martin[26]; see also Ref. 1).

Thomas *et al.*[6] used the absorption coefficient[32] of the excitons (two-particle bound state) as a measure of their density of states $\mathfrak{D}_2$ according to

$$\mathfrak{D}_2(\epsilon) = \alpha_2(\epsilon)/\alpha_0 , \tag{5}$$

with α_0 a constant determined by equating $\lim_{\epsilon\to 0}\alpha_2(\epsilon)$ to the theoretical density of states at the band edge, corrected for experimental resolution $\langle\!\langle\ \rangle\!\rangle_R$, according to

$$\alpha_0 = \frac{\lim_{\epsilon\to 0}\alpha_2(\epsilon)}{\langle (g_2/2\pi^2)(2m_2/\hbar^2)^{3/2}\epsilon^{1/2}\rangle_R} , \tag{6}$$

where $g_2 = 16$ and $m_2 = 0.335 m_0$. [Kamerman and Feldman[33] have used a calculated $\mathfrak{D}_2(\epsilon)$ (Ref. 34) in a similar procedure.] Fitting both the exciton and the e-h liquid line shapes in the ways described above provides us with the energy position of the chemical potential μ' (at the upper edge of the liquid line) and also the bottom of the exciton band ϵ_2', with their difference defined as $\phi(T)$. The temperature dependence of ϕ arises only because μ' is temperature dependent,[17] since the small changes in ϵ_2' due to collision broadening are negligible.[6]

At suitably low temperatures, Eq. (1) can be applied to the gas with the inclusion of only one term, that due to the excitons. Below, we shall generalize this result to extend the calculation to temperatures above 5 K. For the exciton gas the density of states is given by Eqs. (5) and (6). The distribution function is the Bose-Einstein function, but at the low densities that we consider here, the Boltzman and Bose-Einstein functions are indistinguishable. The characteristic energy is $-\phi(T)$ as noted above, so that $f_2(\epsilon + \phi(T)) = \exp[-(\epsilon+\phi)/kT]$. Using these results in Eq. (1) we have calculated the solid line in Fig. 3, as has been done previously,[6] using $\phi(T) = 1.8 + 2.2(k_B T)^2$meV.

The position in density of the exciton phase boundary depends exponentially on the value of ϕ. Since a wide range of values has been reported,[1] we shall review them briefly. We shall not use the values obtained by a direct analysis of low-temperature ($T < 4.2$ K) onsets and decay kinetics of the e-h liquid (Pokrovskii,[35,36] Hensel *et al.*,[37] Lo *et al.*,[38] McGroddy *et al.*,[39] Gershenzon *et al.*,[40] Timusk,[11] Benoit à la Guillaume *et al.*,[41] Westervelt *et al.*,[42] and Fujii and Otsuka[43]), but rather the more detailed analyses of this type of measurement in terms of supersaturation effects (Westervelt *et al.*[44] and Etienne *et al.*[45]) which give

the value[44] of $\phi = 1.9 \pm 0.2$ meV, consistent with (but, we believe, less accurate than) the spectroscopic measurements. Approximate analyses of the exciton line and its position relative to the e-h liquid by Benoit à la Guillaume and Voos,[31] by Lo,[38] and by Martin[27] gave values of $\phi(0) = 2.0$, 2.06 ± 0.15, and 2.25 ± 0.15 meV. An analysis using measured values of the absorption coefficient by Thomas *et al.*[17] gave $\phi(0) = 1.8 \pm 0.2$ meV and a comparable analysis by Kamerman and Feldman[33] using the theoretical density of states of Lipari and Alterelli[34] gave $\phi(0) = 1.9 \pm 0.2$ meV. Although we have used $\phi(0) = 1.8$ meV in Fig. 3, we also show the gas phase boundary for $\phi(0) = 2.0$ meV by the long-dashed line.

An important aspect of the supersaturation effects mentioned above, for purposes of constructing the phase diagram, is that they are reduced at higher temperatures. Consequently, we expect that the "equilibrium" phase boundary will be closer in density to that determined from onsets as the temperature is raised. This coincidence is a necessary assumption in the normalization of the onsets in Fig. 3 with the calculated, equilibrium gas density at $T = 5.5$ K.

Based on the liquid densities above $n \simeq 10^{17}$ cm^{-3} and the gas densities below $n = 10^{15}$ cm^{-3}, Thomas *et al.*[6] suggested that there were probably substantial deviations from the phase diagram of simple fluids. Thomas[10] has reiterated this point and in our work here our major result is the confirmation of this conclusion based on an interpretation of the entire density range. In the context of the various measured values of $\phi(0)$ discussed above, we note that if a larger value of $\phi(0)$ is chosen, the deviation from the simple fluids phase diagram will be larger than that shown in Fig. 3.

We turn now to the extension of the gas phase boundary above $T \sim 5$ K. Thomas, Rice and Hensel[5] noted that, along this boundary, the luminescence line from the gas began to differ from that expected for excitons at $n \sim 4 \times 10^{15}$ cm^{-3}, as indicated by the fact that the lower edge of the line moved to lower energy at higher density (see Fig. 3 of Ref. 5). They also noted that this density is of the order of the Mott density calculated using Debye-Hückel screening.

The Mott density is conceptually crucial to our understanding of the phase diagram. As discussed by Brinkman and Rice[46] and by Rice[4] in the context of the electron-hole fluid, a first-order phase transition should occur at $T = 0$ at a density where the screening length is of the order of the exciton Bohr radius. For the degenerate statistics which hold $T = 0$, the Fermi-Thomas screening length gives a Mott density $n_{\text{Mott}} = (3/4\pi)/(9.9a_X)^3 = 1.7 \times 10^{14}$ cm^{-3}, as indicated by the arrow labelled n_{Mott} in Fig. 3.

An interesting possibility is that this concept could be extended to finite temperatures with the result that two critical points appear as discussed by Landau and Zeldovich.[2] Since the temperatures and densities of interest for the e-h fluid are such[5] that the e-h gas turns out to be nondegenerate, Debye-Hückel screening needs to be considered.

The Debye-Hückel screening wave vector q_D can be written

$$q_D = [8\pi(E_{X0}/k_B T)a_X n^{\pm}]^{1/2}, \tag{7}$$

where here, as below, we shall assume that the characteristic length and energy for the screening by the electrons, holes and trions (whose density sum is $n^{\pm} = n_e + n_h + n_{T^-} + n_{T^+}$) are those of the exciton. The exciton ionization energy at zero density E_{X0} is related to the exciton Bohr radius a_X by

$$E_{X0} = \frac{m_2 e^4/\kappa^2}{2\hbar^2} = \frac{e^2/\kappa}{2a_X}, \tag{8}$$

where[1] $E_{X0} = 4.15$ meV, $m_2 = 0.335 m_0$, and $a_X = 114$ Å for Ge. Using Mott's most recent evaluation[3] of the screening wave vector q_M at the metal-insulator transition, we would expect the disappearance of bound states at $q_M a_X = 1.19$; or using q_D and solving for the Mott density n_M, extended to $T > 0$,

$$n_M = (k_b T/E_{X0})11\pi a_X^3. \tag{9}$$

However, we find, as discussed previously by Thomas and Rice,[14] that the luminescence from the gas above this density cannot be fit with the line shape for the recombination of electrons and holes from parabolic bands.

The luminescence line shape *can* be rather well fit by a combination of excitons and trions. This surprising result presents a serious dilemma in analyzing the gas densities in the region above n_M because none of the theories involving bound states should be applicable. We shall adopt an *ad hoc* resolution of this problem by assuming that a suppression of the effects of screening occurs that is sufficient to move the metal-insulator transition density to values substantially above n_M. We shall then proceed to analyze the thermodynamics of the gas using bound states and assuming that the (reduced) screening effects only produce rigid energy shifts in the bands.

In order to parametrize the observed apparent reduction in screening we shall use the formula of Ebeling, Kraeft, and Kremp[7] for the band gap reduction relative to the exciton band edge. These authors approximated the infinite series of screening terms that contribute to this reduction by a correction which is physically like an ineffectiveness of the Debye-Hückel screening at high densities because of the deBroglie thermal wavelength, which we define as

$$\Lambda = 2a_x(\pi E_{X0}/k_B T)^{1/2}. \quad (10)$$

The exciton ionization energy is then given by

$$E_X(n^\pm) = E_{X0}[1 - 2q_D a_X/(1 + c\Lambda q_D)], \quad (11)$$

where c is a constant which we shall consider to be an arbitrary number to explain the apparent persistence of bound states above n_M. Ebeling *et al.*[7] have estimated the value of c to be $\frac{1}{8}$ in their approximate calculation. In any case, the theory for $E_X(n^\pm)$ is valid only for $n^\pm \ll n_M$ although we shall use the formula primarily at densities near and above n_M. We can solve for the density n_{MI} at which E_X goes to zero to obtain an estimate of the metal-insulator transition that is implied by our parametrization:

$$n_{MI} = \frac{(k_B T/E_{X0})/32\pi a_X^3}{(1 - c\Lambda/2a_X)^2}. \quad (12)$$

Since the densities near $T = 6$ K are important in our attempts to understand the phase diagram, let us evaluate n_{MI} at this point in order to consider the influence of the constant c. Here, $k_B T/E_{X0} = \frac{1}{8}$ and $\Lambda = 10a_X$, so that $2q_D a_x = 1.11(n^\pm \times 10^{15})^{1/2}$ and

$$n_{MI}(6\text{K}) = 8.1 \times 10^{14}\ \text{cm}^{-3}/(1 - 5c)^2. \quad (13)$$

We see that n_{MI} is sensitive to the value of c and is singular at $c = \frac{1}{5}$. Thomas and Rice evaluated Λ for slightly different parameters and, for their choice, n_{MI} becomes infinite at $c = 0.38$. Using the same numerical values as in our n_{MI}, we can plot $E_X(n^\pm)$ as an illustration of the influence of the deBroglie wavelength correction. In Fig. 6 we show E_X as a function of $n^\pm$ for $c = 0$, $\frac{1}{8}$, and $\frac{1}{6}$. We see that with increasing c, n_{MI} becomes greater than n_M as apparently required by our data and we note that $c = \frac{1}{6}$ is of the right order for our data and that of Thomas and Rice.

Under the assumptions that we have bound states above n_M and that we can describe $E_X(n^\pm)$ in an approximate, empirical way, we can then calculate the gas side of the phase boundary for the e-h fluid. For this case, in which there are significant numbers of correlated e-h pairs, excitons, trions, and molecules, we calculate the total density as a sum of several contributions using Eq. (1). We shall use densities of states of the form

$$\mathfrak{D}_j(\epsilon) = (g_j l_j/2\pi^2)(2m_j/\hbar^2)^{3/2}\epsilon^{1/2}, \quad (14)$$

and distribution functions of the form

$$f_j(\epsilon - \mu + \epsilon_{0j}) = \exp[(-\epsilon_j + j\mu/2)k_B T, \quad (15)$$

where the values of the parameters are given in Table I. We shall use $E_X(n^\pm)$ with $c = \frac{1}{6}$ as discussed above. In this way we can extend the calculated equilibrium position of the gas phase boundary to higher density from the low-density region where excitons predominate. The result of this calculation is shown as the dashed line at high gas densities in Fig. 3. The presence of particles other than excitons becomes discernible for temperatures above about 5.5 K. The curve is seen to coincide rather well with the onset measurements up to nearly 6 K. Although this calculation extends the gas boundary somewhat, it is doubtful for $n \gtrsim 10^{16}$ because the screening effects are even larger. However, this result does cover the region near the Mott density as determined from the simple Debye-Hückel screening length and quantitatively describes the apparent absence of a Mott transition. Combining all the results discussed, we find the critical point to be at $T_c = 6.7 \pm 0.2$ K and $n_c = (6 \pm 1) \times 10^{16}$ cm^{-3}.

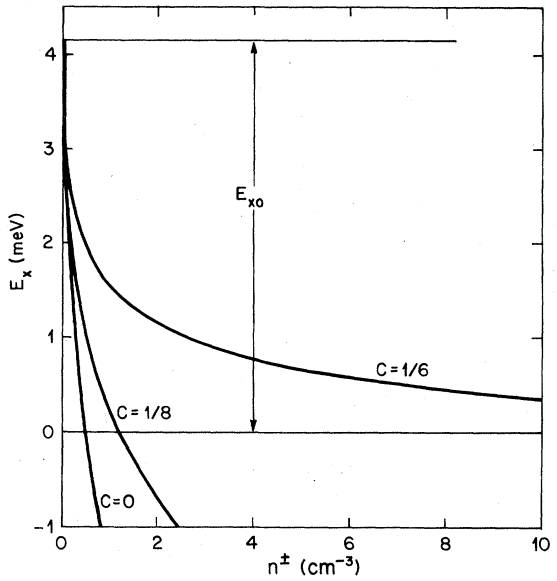

FIG. 6. Theoretical variation of the exciton ionization energy as a function of the density of charged particles for different magnitudes of the screening reduction due to the particles' de Broglie wavelength as discussed in the text. The heavy dashed part of the phase diagram in Fig. 3 is obtained using $E_X(n^\pm)$ with $c = \frac{1}{6}$.

TABLE I. Values of g_j and m_j are approximate values assuming the predominance of heavy holes and the geometric mean of values of g_j for positive and negative particles. The entries l_j are the numbers of e-h pairs in the jth type of complex, counting both positive and negative particles.

j	Particle	g_j	l_j	m_j	ϵ_j^0
1	Electrons and holes	4	1	0.28	$E_X/2 = 24$ K
2	Excitons	16	1	0.335	0
3	Trions	$8\sqrt{7}$	3	0.615	$E_X/2 - E_T = 22$ K
4	Biexcitons	28	2	0.67	$-E_M = -2$ K

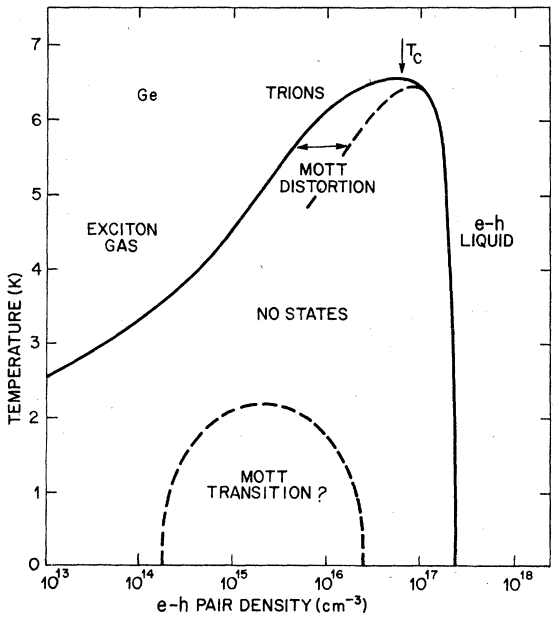

FIG. 7. Phase diagram of the *e-h* fluid in Ge. This plot summarizes the results of Fig. 3. The anomalously low density in the gas near the critical point, compared to that in simple fluids, is labelled a Mott distortion. This distortion may, in a loose sense, be a remnant of of Mott transition (dashed curve, for example) that is eclipsed by the liquid-gas phase transition. A point of view that is consistent with our measurements and analysis is that the liquid-gas transition *is* the Mott transition, except near T_c.

IV. CONCLUSION

We find that the phase diagram of the electron-hole fluid in optically pumped pure Ge is distorted from that expected for simple fluids as shown in Fig. 3. We reach this conclusion based on a combination of results from a series of experiments on both the *e-h* liquid and the "exciton" gas. The central new approximation which allows us to extend this picture is the observation that the line shape of luminescence from the high density gas can be fit by a combination of excitons, trions, and biexcitons. From the relative numbers of trions compared to excitons, an *ad hoc* description of the density dependence of the ionized carrier band edge can be obtained. This analysis in terms of a dominance by simple bound states above the Mott density is of uncertain validity because it does not treat the strong interactions that may distort the densities of states. However, it allows us to put forward a quantitative presentation of our results.

For the composition of the gas given by our fit to the luminescence line, we have written the phase boundary which follows from a straightforward application of thermodynamics on the same footing as the determination of the *e-h* liquid boundary. However, the phase boundary below the critical region in the high-density gas is uncertain in our view for two reasons. First, the effects of screening at $n > n_M$ remain without an adequate theoretical treatment and require further experimental study. Second, the luminescence line shape and onset data obtained from samples with a severe density gradient provide information that is of unsatisfactory quality near the critical point. Although these factors leave the precise shape of the phase boundary uncertain, it is certainly broader in density near the critical point than previously believed.

We have referred to this broadening as a Mott distortion because of the possibility that the Mott transition and the liquid-gas transition affect each other and that the liquid-gas phase boundary eclipses the metal-insulator phase boundary. Rice[4] has discussed the two characteristic densities of the metal-insulator transition at $T = 0$ which allow us to make the arbitrary sketch shown in Fig. 7. As the density of excitons is increased, their wave function overlap will be sufficient (without the presence of free carriers) to cause an ionization collapse at $n_{MI} = 3/4\pi(2a_X)^3 = 2 \times 10^{16}$ cm^{-3}. This density is shown as the lower edge of the metallic phase in Fig. 7. The second (lower) density is the usual Mott density with Thomas-Fermi screening, where excitons would be able to form due to reduced screening as density is reduced in the metallic phase. This value is shown as the upper edge of the insulating phase. The entire phase boundary for a possible metal-insulator phase separation (dashed line in Fig. 7) sketched from these two densities is, of course, inaccessible experimentally within the liquid-gas density separation region. However, it seems plausible that the Mott distortion as described above might be thought of as resulting from the metal-insulator evolution above the T_c for the Mott transition.

In summary, we have completed a thermodynamic description, based on spectroscopic measurements, of the phase separation associated with the liquid-gas transition in the electron-hole fluid. The liquid is metallic at all densities. The gas evolves gradually from this metallic state near the liquid-gas critical density to an ensemble of bound and ionized states at low densities. As a result of this evolution, loosely termed a metal-insulator "transition," the liquid-gas phase boundary is distorted from that of simple fluids.

*Permanent address: Istituto di fisica G. Marconi, Univ. di Roma, Roma, Italy.

[1]T. M. Rice, in *Solid State Physics 32*, edited by H. Ehrenreich, D. Turnbull and F. Seitz (Academic, New York, 1977); J. C. Hensel, T. G. Phillips, and G. A. Thomas, *ibid.*

[2]The possibility of two critical points was first discussed in the context of fluid Hg by L. D. Landau and G. Zeldovich, Acta Phys. Chim. USSR 18, 194 (1943) [*Collected Works of L. D. Landau*, edited by D. ter Haar (Pergamon, New York, 1965)].

[3]N. F. Mott, *Metal-Insulator Transitions* (Barnes and Noble, New York, 1974).

[4]T. M. Rice, (a) *Proceedings of the Twelfth International Conference on the Physics of Semiconductors, Stuttgart, 1974*, edited by M. H. Pilkuhn (Teubner, Stuttgart, 1974), p. 23; (b) *Proceedings of the Oji Seminar on the Physics of Highly Excited States in Solids, Tomakomai, 1975*, edited by M. Ueta and Y. Nishina (Springer, Berlin, 1976), p. 144.

[5]G. A. Thomas, T. M. Rice, and J. C. Hensel, Phys. Rev. Lett. 33, 219 (1974).

[6]G. A. Thomas, A. Frova, J. C. Hensel, R. E. Miller, and P. A. Lee, Phys. Rev. B 13, 1692 (1976).

[7]W. Ebeling, W. Kraeft, and D. Kremp, *Ergebnisse der Plasmaphysik und der Gaselektronik*, Band 5, edited by R. Rompe and M. Steenbeck (Akademie-Verlag, Berlin, 1976).

[8]Z. A. Insepov, G. É. Norman, and L. Yu. Shurova, Zh. Eksp. Teor. Fiz. 71, 1960 (1976) [Sov. Phys.-JETP 44, 1028 (1976)]; Z. A. Insepov and G. E. Norman *ibid.* 62, 2290 (1972) [*ibid.* 35, 1198 (1972)].

[9]L. M. Sander and D. K. Fairobent, Solid State Commun. 20, 631 (1976).

[10]G. A. Thomas, Nuovo Cimento 39, 561 (1977).

[11]T. Timusk, Phys. Rev. B 13, 3511 (1976).

[12]J. Shah, M. Combescot, and A. H. Dayem, Phys. Rev. Lett. 38, 1497 (1977). Results equivalent to these have been explained in Ref. 14 without assuming the occurrence of a phase transition near n_{MI}.

[13]W. Miniscalco, C. C. Huang, and M. Salamon, Phys. Rev. Lett. 39, 1356 (1977).

[14]G. A. Thomas and T. M. Rice, Solid State Commun. 23, 359 (1977).

[15]H. S. Carslaw and J. C. Jaeger, *Conduction of Heat in Solids* (Oxford U. P., London, 1959).

[16]M. Voos, K. L. Shaklee, and J. M. Worlock, Phys. Rev. Lett. 33, 1161 (1974); A. S. Alekseev, T. A. Astimirov, V. S. Bagaev, T. I. Galkina, N. A. Penin N. N. Sybeldin, and V. A. Tsvetkov, in Ref. 4(a), p. 91; J. C. V. Mattos, K. L. Shaklee, M. Voos, T. C. Damen, and J. M. Worlock, Phys. Rev. B 13, 5603 (1976); R. W. Martin, Phys. Status Solidi B 61, 223 (1974); B. J. Feldman, Phys. Rev. Lett. 33, 359 (1974).

[17]G. A. Thomas, T. G. Phillips, T. M. Rice, and J. C. Hensel, Phys. Rev. Lett. 31, 386 (1973); G. A. Thomas, T. M. Rice, and J. C. Hensel, in Ref. 4(a), p. 105.

[18]Ya. Pokrovskii, A. Kaminskii, and K. Svistunova, *Proceedings of the Tenth International Conference on the Physics of Semiconductors, Cambridge, 1970*, edited by S. P. Keller, J. C. Hensel, and F. Stern, CONF-700801 (USAEC Div. Tech. Info., Springfield, Va., 1970), p. 504.

[19]C. Benoit à la Guillaume and M. Voos, Phys. Rev. B 7, 1723 (1973).

[20]T. K. Lo, Solid State Commun. 15, 1231 (1974).

[21]R. W. Martin and R. Sauer, Phys. Status Solidi B 62, 443 (1974); R. W. Martin, Solid State Commun. 19, 373 (1976).

[22]R. W. Martin, H. L. Störmer, W. Rühle, and D. Bimberg, J. Lumin. 12–13, 645 (1976).

[23]R. W. Martin and H. L. Störmer, Solid State Commun. 22, 523 (1977).

[24]G. A. Thomas and M. Capizzi, *Proceedings of the Thirteenth International Conference on Physics of Semiconductors, Rome, 1976*, edited by F. G. Fumi (Tipographia Marves, Rome, 1976), p. 914.

[25]T. M. Rice, Nuovo Cimento B 23, 226 (1974).

[26]H. Störmer, Ph. D. dissertation (Universität Stuttgart, Stuttgart, 1977) (unpublished).

[27]R. Martin, Ph. D. dissertation (Universität Stuttgart, Stuttgart, 1977) (unpublished).

[28]W. Miniscalco, C. C. Huang, and M. B. Salamon, Phys. Rev. Lett. 39, 1356 (1977).

[29]W. Miniscalco, Ph. D. dissertaion (University of Illinois, Urbana, Ill., 1977), available from University Microfilms.

[30]J. B. Mock, M. Combescot, and G. A. Thomas, Solid State Commun. 25, 279 (1978).

[31]C. Benoit à la Guillaume and M. Voos, Solid State Commun. 12, 1257 (1973).

[32]A. Frova, G. A. Thomas, R. E. Miller, and E. O. Kane, Phys. Rev. Lett. 34, 1572 (1975).

[33]G. W. Kamerman and B. J. Feldman, Phys. Rev. B 15, 1209 (1977).

[34]M. Altarelli and N. O. Lipari, Phys. Rev. B 15, 4883 (1977); 15, 4898 (1977).

[35]Ya. E. Pokrovskii, Phys. Status Solidi A 11, 385 (1972).

[36]Ya. E. Pokrovskii, *Proceedings to the Eleventh International Conference on the Physics of Semiconductors, Warsaw, 1972*, (PWN, Warsawa, 1972), p. 69.

[37]J. C. Hensel, T. G. Phillips, and T. M. Rice, Phys. Rev. Lett. 30, 227 (1973).

[38]T. K. Lo, B. J. Feldman, and C. D. Jeffries, Phys. Rev. Lett. 31, 224 (1973).

[39]J. C. McGroddy, M. Voos, and O. Christensen, Solid State Commun. 13, 1801 (1973).

[40]E. M. Gershenzon, G. N. Gol'tsman, and N. G. Ptitsina, Zh. Eksp. Teor. Fiz. 70, 224 (1976) [Sov. Phys.-JETP 43, 116 (1976)].

[41]C. Benoit à la Guillaume, M. Capizzi, B. Etienne, and M. Voos, Solid State Commun. 15, 1031 (1974).

[42]R. M. Westervelt, T. K. Lo, J. L. Staehli, and C. D. Jeffries, Phys. Rev. Lett. 32, 1051 (1974); 32, 1331(E) (1974).

[43]K. Fujii and E. Otsuka, Solid State Commun. 14, 763 (1974).

[44]R. M. Westervelt, J. L. Staehli, E. E. Haller, and C. D. Jeffries, in Ref. 4(b), p. 270; R. M. Westervelt, Phys. Status Solidi B 74, 727 (1976); R. M. Westervelt, *ibid.* 76, 31 (1976); J. L. Staehli, *ibid.* 75, 451 (1976); R. M. Westervelt, in Ref. 24, p. 902.

[45]B. Etienne, C. Benoit à la Guillaume, and M. Voos, Nuovo Cimento 39, 639 (1977); and Phys. Rev. B 14, 712 (1976).

[46]W. F. Brinkman and T. M. Rice, Phys. Rev. B 7, 1508 (1973).